International Journal of Thermophysics, Vol. 14, No. 1, 1993

Estimation of Thermophysical Properties of a Film Coated on a Substrate Using Pulsed Transient Analysis

S. W. Kim[1] and R. E. Taylor[2]

Received September 8, 1992

The thermophysical properties (thermal diffusivity, effusivity) of a film coated on a substrate have been measured by a pulsed transient analysis. The experimental approach is to utilize the film surface temperature decay following a heating pulse from a Q-switched Nd:glass laser. The temperature decay was measured using a HgCdTe infrared detector. Following the collection of data, a nonlinear least-squares regression was performed to estimate the optimal values of three separate thermal parameters by fitting the data to the semiinfinite substrate model solution. The model was checked systematically by analysis of the sensitivity and correlation of the three parameters, and the thermal diffusivity and effusivity ratio of the film and substrate were obtained from the optimal values of the estimated parameters.

KEY WORDS: thermal diffusivity; film; effusivity; parameter estimation; pulsed transient analysis.

1. INTRODUCTION

The understanding of heat transfer through thin film coatings applied to substrates has become increasingly important in technological applications. Such coatings are applied for reasons such as preventing oxidation, protecting against erosion damage, and controlling the thermal and electrical properties of the surface. In many situations, it is not possible to obtain coatings as independent samples separate from their substrates.

[1] Temperature Laboratory, Korea Research Institute of Standards and Science, P.O. Box 3, Taedok Science Town, Taejon 305-606, Republic of Korea.

[2] Thermophysical Properties Research Laboratory, School of Mechanical Engineering, Purdue University, West Lafayette, Indiana 47906, U.S.A.

0195-928X/93/0100-0135$07.00/0

Since its inception in 1961 by Parker et al. [1], the flash method has achieved a worldwide status as a standard technique for the measurement of thermal diffusivity of solids. Unfortunately, this method has been unsuccessful in the case of a highly conducting film applied to a thick, less conducting substrate. In this situation, the heat diffusion time through the film is substantially less than through the substrate, and as a result, the film has little effect on the temperature rise of the rear surface.

The objective of this work is to utilize a technique that can easily distinguish the influences of the film layer and the film–substrate interface on the heat conduction transient. The analysis is based on the one-dimensional heat conduction equation for a very short-duration heat pulse on the front surface at time 0. Unlike the traditional rear surface temperature rise curve, the front film surface temperature decay is measured. This technique is well suited for thin films applied to thick substrates because the effects of the layers and their interface are time resolved [2–4]. By the data analysis using the parameter estimation technique [5], the reliability of this model was systematically checked and the thermal diffusivity of films and the effusivity ratio of the film and substrate were determined.

2. TRANSIENT ANALYSIS IN A FILM–SUBSTRATE SYSTEM

In this work, it is proposed to utilize the front surface temperature decay rather than the rear surface temperature rise. The advantage of using this technique is that the effect of each layer and the interface between the layers is time resolved. The model for the surface temperature decay in two-layered composites has already been developed, but the solution contains a complicate transcendental equation which is due to the finite substrate thickness [2].

2.1. A Semiinfinite Substrate Model

In simplifying the solution of a two-layer composite temperature transient, the primary assumption is that the substrate is considered as a semiinfinite medium. This assumption is valid provided that the heat wave does not approach the rear surface of the substrate during the required duration of the experiment. It will be shown that the experimental duration required is that which is long enough to allow for a portion of the heat flux to transmit through the interface of the film and the substrate. The diagram showing the two-layer, semiinfinite substrate model is shown in Fig. 1.

In developing the film surface temperature decay, the primary assumptions are [6] as follows:

(1) heat flow in the x-direction is one-dimensional,
(2) all thermal properties are constant,
(3) both layers are homogeneous,
(4) the substrate is a semiinfinite medium,
(5) the heat pulse is uniformly absorbed on the front surface,
(6) there is no interfacial contact resistance, and
(7) there are no heat losses from the composite specimen.

Taking the Laplace transforms of the heat diffusion equations for each layer, and equating the temperature of each layer according to the interface conditions, the solution for the surface transient temperature, $U(0, t)$, can easily be determined. Because the measurement system utilizes a Q-switched laser, it is assumed that the applied heat pulse is instantaneous in comparison to the duration of heat propagation, allowing for the use of the Dirac pulse input. For this situation, the solution is simple and is given as follows [6]:

$$U(0, t) = \frac{q}{e_f \sqrt{\pi t}} \left[1 + 2 \sum_{i=1}^{\infty} \sigma^i \exp\left(\frac{-i^2 b^2}{\alpha_f t} \right) \right] \tag{1}$$

where

$U(0, t) = T - T_0$, the film surface temperature excursion from the initial temperature

q = energy constant absorbed at film surface

$e_{12} = e_f / e_s$, effusivity ratio

$e_f = (k_f \rho_f C_{pf})^{1/2}$, film effusivity

$e_s = (k_s \rho_s C_{ps})^{1/2}$, substrate effusivity

$\sigma = (e_{12} - 1)/(e_{12} + 1)$

α_f = film thermal diffusivity

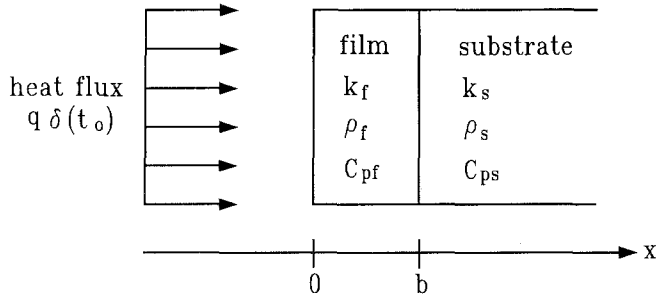

Fig. 1. Diagram of a two-layer semiinfinite substrate model.

The variable σ is an important term, as it is the only term which contains information pertaining to the substrate and the substrate's relation with the film. The physical range of σ is $(-1 \leqslant \delta \leqslant 1)$, where a positive value represents a conductive film applied to an insulative substrate, and a negative value represents an insulative film applied to a conductive substrate.

Figure 2 shows a logarithmic plot of Eq. (1) for a two-layer semi-infinite specimen with the spectrum of σ values. The slopes of the curve indicate the rate variation of heat transfer from the front surface to the substrate. For the cases of $\sigma > 0$, the slope of the temperature decaying curve changes from higher to lower values after the turning point, and for the case of $\sigma < 0$, the slope changes from lower to higher values. As shown in Fig. 2, the turning point occurred due to the interface of two different materials.

2.2. Nonlinear Response of the Detector to Temperature

The signal of the infrared detector is not always linearly proportional to the actual surface temperature [7, 8]. If it is assumed that the proportion is nonlinear, the output voltage of the detector can be expressed as follows:

$$E = CT^n \tag{2}$$

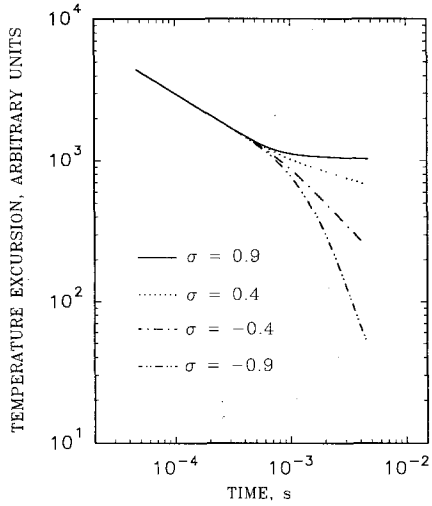

Fig. 2. Temperature excursion of the film surface represented by Eq. (1) for various values of σ.

where E is the voltage of the detector, n is the detector power constant, and C is a proportional constant which depends on many factors such as the film emissivity, voltage sensitivity of the detector, and angular aperture of the detector [9]. Writing Eq. (2) for the surface temperature as a function of time and also for the initial constant value previous to the energy pulse results in the following two equations:

$$E(t) = C[T(t)]^n \tag{3}$$

$$E_0 = CT_0^n \tag{4}$$

Dividing Eq. (3) by Eq. (4), using Eq. (1), and rearranging the terms results in the following equation:

$$T_0\left[\left(\frac{E(t)}{E_0}\right)^{1/n} - 1\right] = U(0, t) \tag{5}$$

In Eq. (5), the constant C, which is difficult to determine, has dropped out. The value of n can be deduced from the decay curve in the region where the film is in its semiinfinite region.

3. PARAMETER ESTIMATION

Parameter estimation (PE) is a powerful technique that uses all the available data points and provides statistical means to analyze the experiment [5, 10]. Parameter estimation procedure was the method of choice to get optimum values for the unknown terms governed by Eq. (1). In this work three parameters are defined as follows:

$$\beta_1 = \alpha_f / b^2 \tag{6}$$

$$\beta_2 = e_{12} \tag{7}$$

$$\beta_3 = q/(e_f\sqrt{\pi}) \tag{8}$$

A nonlinear PE algorithm, NL2SOL, developed by Dennis et al. [11, 12], was used in this work. The reliability of the estimated parameters obtained by using NL2SOL software depends on the sensitivity coefficients (SC) of each parameter.

The SCs for the parameters can provide a considerable amount of insight as to the adequacy of the model [10]. If the model behaves similarly with a change in one parameter as it does with a change in another parameter, then the parameters are correlated, or dependent to some degree.

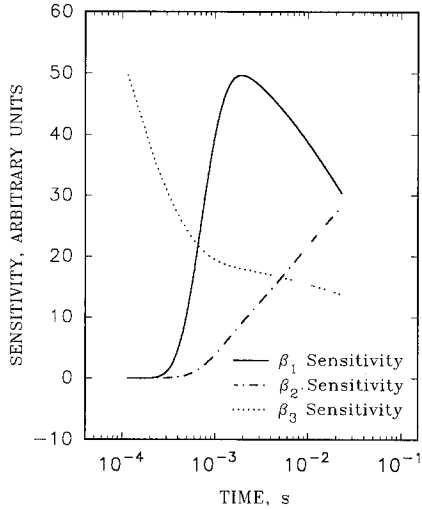

Fig. 3. Calculated SCs for a positive σ value when $\beta_1 = 431.9\ s^{-1}$, $\beta_2 = 9.0$, and $\beta_3 = 30.0$ (arbitrary units).

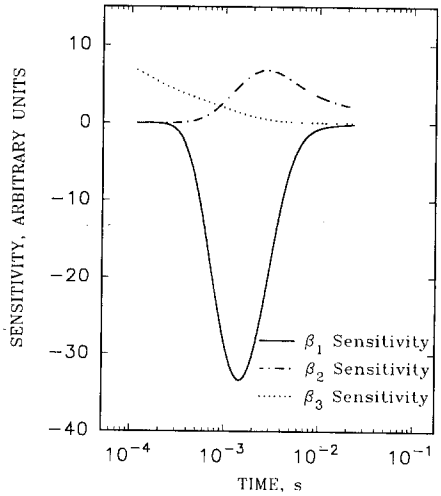

Fig. 4. Calculated SCs for a negative σ value when $\beta_1 = 431.9\ s^{-1}$, $\beta_2 = 0.11$, and $\beta_3 = 30.0$ (arbitrary units).

Table I. Calculated Values of Correlation Coefficients with Different σ Values

σ	$\beta_1\beta_2$	$\beta_1\beta_3$	$\beta_2\beta_3$
0.9	−0.772	−0.645	0.086
0.7	−0.746	−0.605	0.019
0.5	−0.725	−0.567	−0.027
0.3	−0.710	−0.532	−0.053
0.1	−0.700	−0.502	−0.061
−0.1	0.707	0.471	−0.039
−0.3	0.696	0.451	−0.022
−0.5	0.694	0.432	0.014
−0.7	0.694	0.418	0.063
−0.9	−0.696	0.408	0.123

Figure 3 presents the calculated SCs for the case of positive σ values when $\beta_1 = 431.9\ s^{-1}$, $\beta_2 = 9.0$, and $\beta_3 = 30.0$ (arbitrary units). Both the β_1 and the β_2 SCs show the increasing trend with time, but the β_3 SC is a decreasing function. From these it can be assumed that β_1 and β_2 are dependent to each other to some degree, but β_3 is nearly independent of β_1 and β_2. Figure 4 presents the calculated SCs for the case of negative σ values when $\beta_1 = 431.9\ s^{-1}$, $\beta_2 = 0.11$, and $\beta_3 = 30.0$. All of the SCs look like different functions of time. However, the SCs of β_1 and β_2 show the quasi-symmetry relation. This indicates that β_1 and β_2 are dependent to some degree, but β_3 is nearly independent of the others.

The correlation coefficient (CC) is a quantitative measure of how β_j and β_k are related (β_j and β_k are the ith parameters) [10]. The CC physically has the range of $(-1 \leqslant \rho_{jk} \leqslant 1)$, where ρ_{jk} is the CC of β_j and β_k. The significance of ρ_{jk} is that it describes the degree of linear dependency of the two parameters. Completely linear dependency is implied when ρ_{jk} approaches ± 1. Table I shows the calculated values of CC with different values of σ. β_1 is highly correlated with β_2 and moderately correlated with β_3, and β_2 is quite independent from β_3. The absolute values of CC for all the positive σ are slighly larger than those for all the negative σ. This indicates that the adopted model is more reliable for the negative cases (insulative film applied to a conductive substrate cases).

4. EXPERIMENT

4.1. Preparation of Specimens

The specimens used are comprised of homogeneous film layers applied to homogeneous substrates. The thicknesses of the films were determined

either by direct measurement using a micrometer or by the combination of their weight, density, and geometry. The diameters of all the specimens were 0.5 in., and Table II summarizes the specimen materials and film thicknesses. The specimens which have an epoxy substrate were fabricated by forming a cylindrical mold on the back of a clean metal foil and then pouring 5-min epoxy resin in the mold. The epoxy used was manufactured by Devcon. The metal foils were first slightly roughened and then cleaned to allow for a good contact with the epoxy substrate.

The specimens consisting of graphite films were prepared using Cotronix 931 graphite adhesive coating. The adhesive coating consists of very small graphite particles mixed with a small amount of adhesive cement. The graphite adhesive was applied to the substrates, which were first cleaned and weighed. Following the application, the specimens were cured at 100°C for 16 hr. The graphite coating was then carefully sanded to the desired thickness. The uniformity of the thickness was maintained by periodically checking point thickness with a micrometer. The final thickness was determined by using the weight change, due to the addition of the coating, the density, and the surface area geometry. The thicknesses of all the specimens including the substrate were about 10 mm.

4.2. Experimental Apparatus

The experimental apparatus consists of five major components: a Q-switched Nd: glass laser, a laser sensing photocell, a cavity to hold the specimen and reduce convection losses as well as stray radiation, an infrared detector focused on the specimen, and a digital data acquisition system which consists of a digital oscilloscope in direct communication with a personal computer. A schematic of the system is shown in Fig. 5. The heat pulse is generated using the laser system to produce a

Table II. Two-Layer Specimen Descriptions

	Film coating		
Specimen No.	Material	Thickness (mm)	Substrate material
1	Copper	0.51	Epoxy resin
2	Aluminum	0.82	Epoxy resin
3	304 SS	0.27	Epoxy resin
4	Graphite	0.30	Aluminum
5	Graphite	0.35	Copper

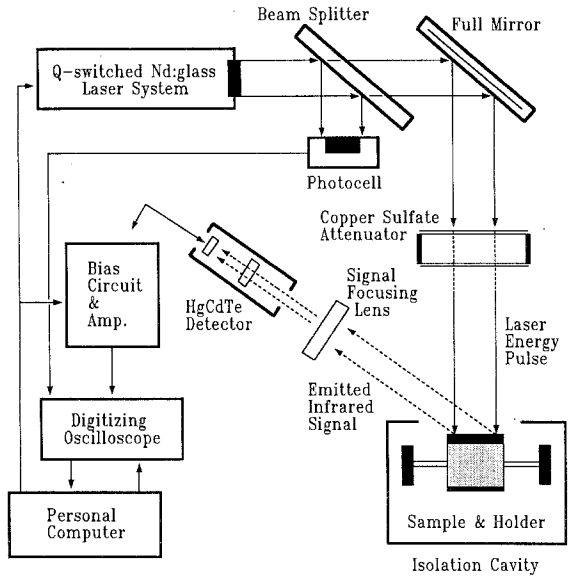

Fig. 5. Functional diagram of the experimental apparatus.

monochromatic beam of energy. This energy is then uniformly applied to the entire surface of the film. The temperature of the film is continuously monitored by the infrared detector, which is also focused directly on the surface of the film but at an angle from the laser beam. The output of the detector is then monitored with the digital oscilloscope. A small portion of the laser energy is deflected onto a photocell which is used to trigger the oscillosope.

The beam diameter of the laser is 0.5 in., the wavelength is 1.06 μm, the pulse duration is 50 ns, and the linewidth is 0.4 Å. The energy of the laser beam is controlled by varying the concentration of a solution of copper sulfate which is placed in line with the laser beam. The detector used to sense the temperature change is a liquid nitrogen-cooled HgCdTe infrared detector with an operating wavelength band between 3.0 and 14 μm. The specified detectivity is $3.7 \times 10^{10}\,\text{mm} \cdot \text{Hz}^{1/2} \cdot \text{W}^{-1}$, with an active area of 1 mm^2. The output of the detector is amplified using an operational amplifier which has a bandwidth of approximately 2 MHz. A ZnSe lens is used to focus the specimen's surface on the detector's active area in order to gain maximum signal with little interference as possible. In addition, a laser wavelength (1.06 μm) band notch filter is used to eliminate any possible detection of reflected laser beam energy.

4.3. Data Reduction

The collected data are plotted on a log(time) vs log(voltage) scale to verify that the experiment was performed in the substrate's semiinfinite regime. Data that represent establishment of the steady-state condition, where the substrate's rear surface influences the heat propagation, are discarded. In the situation of detector nonlinearity as mentioned in Section 2.2, the slope in the semiinfinite film region is $-n/2$, where n is the detector power constant in Eq. (2). The program calculates the slope of the semiinfinite film data and linearizes the data according to Eq. (5). Following this, the data are analyzed. The program uses all of the user-supplied information to select the appropriate data points for use in the analysis and an initial setting value for the parameters.

4.4. Sources of Errors

There are several factors which can be the sources of experimental errors as follows [6, 13]:

(1) finite response of the detection system,
(2) finite pulse time effect of the laser beam,
(3) spatial nonuniformity of the laser beam, and
(4) convection heat loss from the specimen.

The first two effects are not significant in the present work because the time duration for the heat pulse to pass the films is of the order of milliseconds and it is much longer than the response time of the detector (microsecond order) and the pulse duration (nanosecond order).

The modeling of nonuniform heating is a difficult task due to the complexity of the surface temperature distribution followed by a laser heating pulse, and the effect of the factor (3) is not negligible, however, quantitative investigation of this effect is not performed at this time. For more detailed investigation of this effect, a three-dimensional heat conduction analysis is required. If the specimen is placed in a vacuum, the convection heat loss can be negligible.

5. RESULTS AND DISCUSSION

The experiments were performed five times for each specimen. As predicted in Fig. 2, for specimens 1–3 ($\sigma > 0$ cases), the slope of the temperature decay curve changes from high to low values after the turning point, and for specimens 4 and 5 ($\sigma < 0$ cases), the slope changes from low to high values. Figures 6 and 7 show the measured temperature excursion

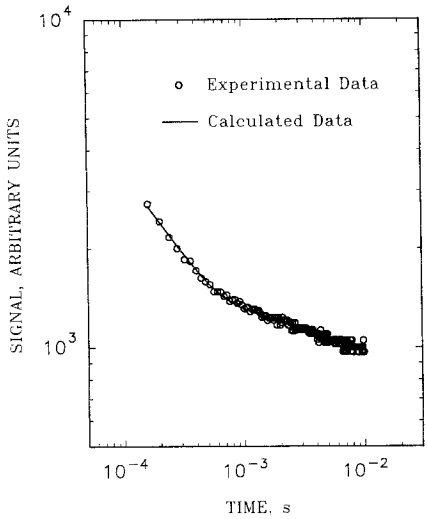

Fig. 6. Experimental data on the temperature excursion of the surface with the theoretical curve fit using the parameter estimation for specimen 1.

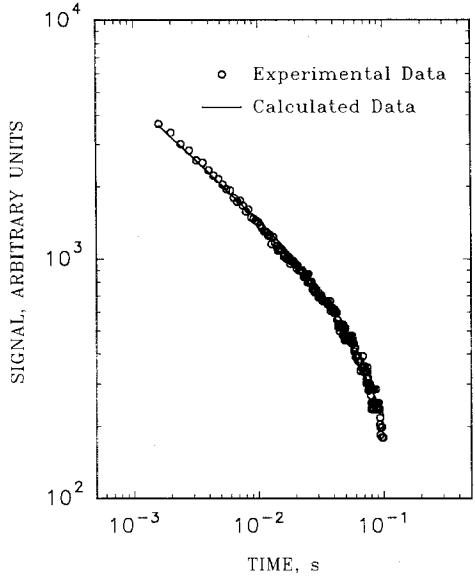

Fig. 7. Experimental data on the temperature excursion of the surface with the theoretical curve fit using the parameter estimation for specimen 5.

Table III. Thermal Diffusivity Values and Effusivity Ratios Obtained in this Work Compared with the Values Quoted in the Literature [14, 15]

Specimen No.	α_f ($cm^2 \cdot s^{-1}$)		Diffusivity difference (%)	e_{12}		e_{12} difference (%)
	Measured	Literature		Measured	Literature	
1	1.21 ± 0.11	1.123	+7.4	68.3	87.2	−21.7
2	0.91 ± 0.08	0.970	−6.2	38.7	46.1	−16.1
3	0.037 ± 0.003	0.039	−5.1	12.5	14.2	−12.0
4	0.018 ± 0.001	0.017	+5.9	0.054	0.050	+8.0
5	0.016 ± 0.002	0.017	−5.9	0.028	0.026	+7.7

for specimen 1 and specimen 5 after linearization, respectively. The calculated data curves were obtained by using the three parameter estimation procedure.

Table III compares the results of the data analysis for five specimens with values from open literatures. The thermal diffusivities obtained from optimum values of β_1 show a reasonably good agreement (5–7%) with the literature values [14, 15]. This is because the thermal diffusivity of the film is determined from the information that the slopes of the curve of the temperature excursion showed a significant change due to the interface of two different materials. However, the effusivity ratio, e_{12}, obtained from β_2 shows larger differences (8–22%) from the literature values compared to the thermal diffusivity. This behavior can be explained reasonably by convection heat losses.

For the positive σ specimens, because the temperature change per unit time is small in the later portion of the thermal decay, as opposed to the earlier portion, it is expected that the heat losses influence the curve primarily in the latter portion. The negative deviation from the literature value indicated for specimens 1–3 means that the latter portion of the experimental curve was forced to decay faster than expected. For specimens 4 and 5 ($\sigma < 0$ case), because the temperature change per unit time is small in the earlier portion of the thermal decay, it is expected that the heat losses influence the curve primarily in the earlier portion. The positive deviation indicated for specimens 4 and 5 means that the earlier portion of the experimental curve was forced to decay faster than expected.

Specimen 1, which has the largest difference in thermal diffusivity between the two composing materials, shows the largest deviation of e_{12}. This means that the contact resistance affects the data to some degree and this should be considered.

6. CONCLUSIONS

The thermal properties of films applied to the substrates were determined by a pulsed transient method. The obtained thermal diffusivity values are in reasonably good agreement (5–7%) with the literature values. Because of the convection heat losses, the effusivity ratio obtained shows larger deviations (8–22%) from the literature values. If the specimen is placed under vacuum or the heat losses are considered in the theoretical model, the results are likely to be improved. The results indicate that this technique has a great potential in the measurement of the thermal diffusivity of thin films. For more advanced analysis, the effects of convection heat losses and contact resistance between two materials should be throughly investigated. Furthermore, the three-dimensional heat transfer model should be adopted.

ACKNOWLEDGMENTS

The authors would like to thank Dr. J. Lee for helpful discussions and Mr. T. R. Goerz for techanical assistance. The first author would like to thank Dr. D. Chi and Mr. J. C. Kim for their technical support and the Korea Science and Engineering Foundation for supporting this study.

REFERENCES

1. W. J. Parker, R. J. Jenkins, C. P. Butler, and G. L. Abbott, *J. Appl. Phys.* **32**:1679 (1961).
2. D. L. Balageas, J. C. Krapez, and P. Cielo, *J. Appl. Phys.* **59**:348 (1986).
3. D. M. Bosher, A. A. Deom, and D. L. Balageas, *High Temp. High Press.* **21**:113 (1989).
4. W. P. Leung and A. C. Tam, *J. Appl. Phys.* **63**:4505 (1988).
5. J. V. Beck and K. J. Arnold, *Parameter Estimation in Engineering and Science* (Wiley, New York, 1977), Chaps. 2 and 6.
6. J. J. Hoefler, M.S.M.E. thesis (Purdue University, West Lafayette, IN, 1989), Chap. 2, App. C.
7. D. P. H. Hasselman and K. Y. Donaldson, *Int. J. Thermophys.* **11**:573 (1990).
8. J. J. Hoefler and R. E. Taylor, *Int. J. Thermophys.* **11**:1099 (1990).
9. P. Cielo, *J. Appl. Phys.* **56**:230 (1984).
10. S. W. Kim, J. Lee, and R. E. Taylor, *Int. J. Thermophys.* **12**:1063 (1991).
11. J. E. Dennis, Jr., M. D. Gay, and R. E. Welsch, *Trans. Math. Software* 7:348 (1981).
12. J. E. Dennis, Jr., M. D. Gay, and R. E. Welsch, *Trans. Math. Software* 7:369 (1981).
13. W. P. Leung and A. C. Tam, *J. Appl. Phys.* **56**:153 (1984).
14. H. J. Lee, Ph.D.M.E. thesis (Purdue University, West Lafayette, IN, 1975), Chap. 4.
15. F. P. Incropera and D. P. DeWitt, *Fundamentals of Heat and Mass Transfer*, 3rd ed. (Wiley, New York, 1990), App. A.